Date:

Optimal flight parameters for UAV laser scanning in forestry operations, with insights into the effect of understory and stocking on data quality

Summary: This study evaluated how flight and sensor parameters influenced data quality and performance of unmanned aerial vehicle (UAV) laser scanners (ULS) in forestry applications. A controlled trial was conducted using the DJIL1 and DJIL2 UAV-mounted LiDAR systems, and benchmarked against a survey-grade Riegl MiniVUX scanner. Five key performance metrics were assessed against ground truth measurements: tree detection, canopy height model (CHM), digital terrain model (DTM), tree height accuracy, and diameter at breast height (DBH) prediction. Stand conditions, including understory presence and stand stocking, were also considered, as well as operational considerations (point cloud density and flight time efficiency).

Across all performance metrics, flight altitude emerged as the most influential parameter, with lower (60 m AGL) rather than higher flights (120 m) consistently producing more accurate results. LiDAR return type was also critical: using all returns substantially improved DTM, CHM and tree height accuracy compared to the first returns alone. Overlap showed consistent but smaller benefits, with higher overlaps (90%) slightly improving CHM and DBH accuracy. Flight speed had a relatively minor impact, although slower flights occasionally improved canopy-based metrics.

The choice of sensor proved to be the strongest driver of performance across the metrics. DJIL2 consistently outperformed DJIL1 across all metrics and, in many cases, performed comparably to the survey-grade MiniVUX despite being a fraction of the cost. This suggests that DJIL2 is a highly robust and cost-effective option for the forest industry, while DJIL1 can still deliver competitive results when flights are carefully planned.

Site conditions also affected performance. The presence of understory vegetation reduced the accuracy of the DTM, CHM, and tree height estimates, but had minimal influence on tree detection and DBH predictions, which depend more on upper crown structure. Stocking rate influenced outcomes in complex ways: tree detection was most accurate in low-density stands, while CHM, DTM, height, and DBH accuracy improved with higher stand densities. These trends warrant further study to confirm their consistency across a larger dataset and varied forest conditions.

From an operational perspective, flight times were most strongly affected by swath overlap, while point density was driven by a combination of altitude, speed, overlap, and scan rate.

In summary, this study demonstrates that ULS performance in forestry is highly sensitive to flight design, with altitude, overlap, and sensor choice dominating outcomes. The results provide actionable guidance for balancing acquisition efficiency with data quality, supporting broader operational adoption of ULS in forest measurement and monitoring.

Authors: **Robin Hartley, Sadeepa Jayathunga, Heather Harper, Peter Massam, Honey Jane Estarija and Kevin Jae Park.**

Forest Growers Research Ltd, PO Box 1127, Rotorua. Ph: 07 921 1883 Email: forestgrowersresearch@fgr.nz Web: www.fgr.nz

1. Introduction

Traditional forest measurement methods are time-consuming, costly and prone to bias (Apostol, et al., 2007; Larjavaara, et al., 2013). Forestry was one of the earliest sectors to adopt remote sensing, recognising its potential for measuring forests in a more timely and cost-effective manner (Koch, 2016). Of all the techniques, airborne laser scanning (ALS/airborne lidar) has proven to be particularly effective due to its ability to characterise forests in three dimensions (White, et al., 2016). While ALS performs well for area-based k-nearest neighbour and individual tree-based inventories (Vastaranta, et al., 2009), it remains costly at small scales and lacks the resolution required for precise modelling of key individual tree-level metrics such as diameter at breast height (DBH) (Watt, et al., 2024).

The miniaturisation of laser scanners for unmanned aerial vehicles (UAV-LS/ULS) has generated strong interest in forestry, offering the potential for lower-cost, more flexible data collection (Jaakkola, et al., 2010; Kellner, et al., 2019; Wallace, et al., 2012). The recent introduction of industrial-grade ULS sensors has now brought ULS within reach of routine operational forestry applications (Štroner, et al., 2021), such as post-thinning stocking assessment (Irwin, et al., 2025) and inventory (Hartley, et al., 2025).

However, flight settings strongly impact point cloud density and, in turn, the accuracy of derived metrics (Hu, et al., 2020). While research has explored ULS applications in forestry (Watt, et al., 2025), relatively little attention has been given to flight optimisation across a comprehensive range of flight parameters (Hu, et al., 2020). Optimisation studies provide a useful resource to help foresters determine parameters that will help them balance data quality with data collection efficiency (Dhruva, et al., 2024).

In practice, foresters in Aotearoa New Zealand (AoNZ) often rely on trial-and-error flight planning or adopt recommendations from researchers, whose data acquisition settings often prioritise ultra-dense point clouds that are inefficient for routine operations. The absence of clear, optimised flight guidelines creates barriers to operational uptake, with oversampling used to compensate for planning uncertainty, thereby masking the potential efficiency gains ULS can offer.

Objective

The objectives of this study were to:

(i) Identify optimal flight parameters for producing key forestry metrics and spatial products (individual tree detection, CHM, DTM, tree height and diameter at breast height–DBH), using two commonly deployed ULS sensors;
(ii) Compare the performance of these sensors against each other and against a survey-grade benchmark sensor;
(iii) Define a set of best-practice flight parameters that balance accuracy and efficiency across all derived spatial products;
(iv) Assess the influence of understory vegetation on the quality of derived products;
(v) Evaluate the effect of stocking rate (stand density/stems per ha) on the derived metrics and products.

A standard operating procedure (SOP) has also been developed alongside this report to support effective uptake by industry stakeholders.

2. Methods

2.1. Study site

The study was conducted in a ~0.5 ha stand of *Pinus radiata* D. Don located in Scion's nursery in Rotorua, AoNZ (Figure 1). The trial comprised six-year-old trees, planted at an unusually high density of 10,000 stems per hectare (1 x 1 m spacing), as the trial was never intended to reach maturity.

Forest Growers Research Ltd, PO Box 1127, Rotorua. Ph: 07 921 1883 Email: forestgrowersresearch@fgr.nz Web: www.fgr.nz

To make the stand more like a conventional forestry trial, trees were thinned to three different stocking rates – 833 stem/ha (4 x 3 m), 1111 stem/ha (3 x 3 m) and 1667 stem/ha (2 x 3 stem/ha), providing a range of commonly established stocking rates within the AoNZ forestry context.

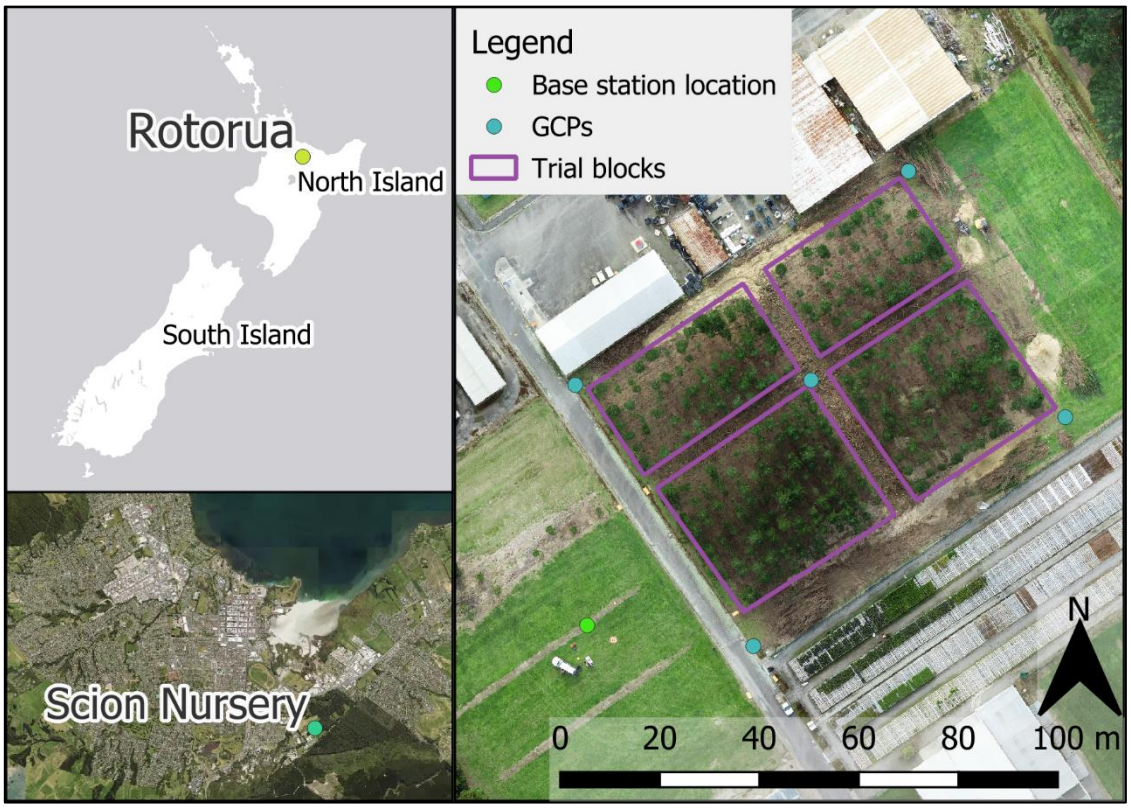

Figure 1. Trial layout: Inset maps show the trial location within AoNZ and Rotorua area, along with an orthomosaic of the trial site. The trial was divided into four blocks (purple polygons) representing different stocking treatments of approximately equal area. The – north-west and north-east blocks (833 stems/ha) were smaller and so combined to match the area of the south-west block (1667 stems/hah) and south-east block (1111stems/ha). Ground control points (GCPs, teal points) and the base station location (green point) are also shown for reference.

To evaluate the impact of understory on the ULS data, all felled trees were left intact beneath the canopy to simulate understory vegetation (Figure 2a). After the first cohort of flights with "understory" present, these were subsequently removed and chipped to leave a forest floor free from understory, and the flights were repeated, enabling comparison of ULS data under conditions with and without understory (Figure 2b).

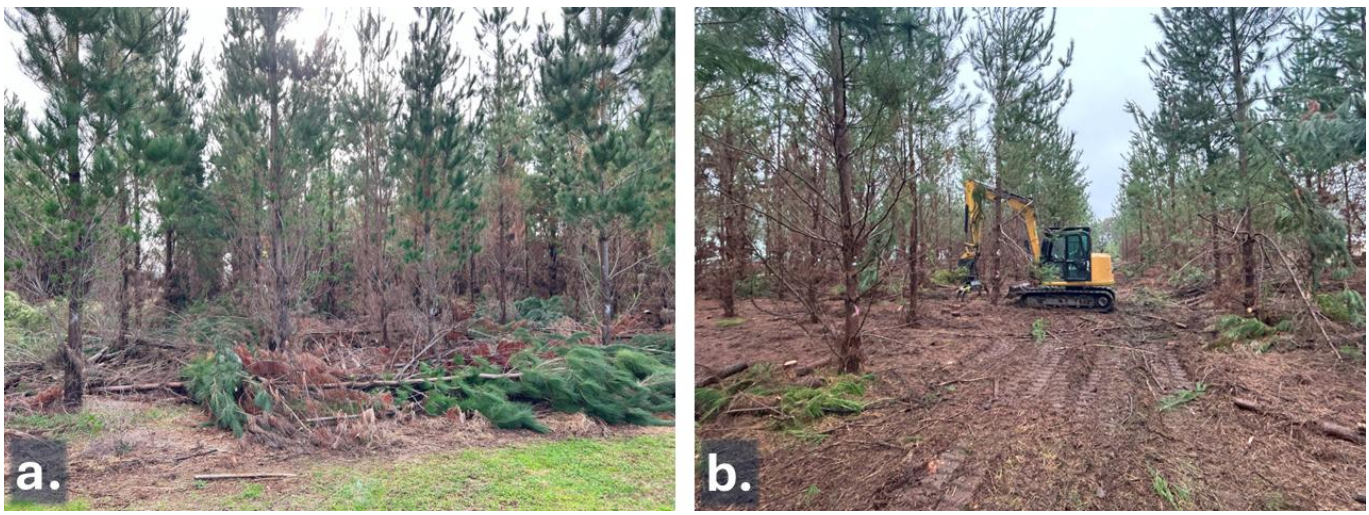

Figure 2. Understory treatments: a. Thinned trees left in-situ to simulate understory and ground cover; b. Site was cleared after the initial cohort of UAV flights to leave an understory-free site.

Forest Growers Research Ltd, PO Box 1127, Rotorua. Ph: 07 921 1883 Email: forestgrowersresearch@fgr.nz Web: www.fgr.nz

2.2. Field data capture methods

Field measurements were collected to provide ground truth data for validating ULS-derived metrics. Tree height was measured using a Vertex V hypsometer, and DBH was measured at 1.4 m above the highest ground adjacent to the base of each tree using a DBH tape with 1 mm precision. In the case of swelling at 1.4 m, the DBH was moved according to standard AoNZ forestry principles, with the new measurement height recorded (CNI Regional YTGEN User Group, 2007). For tree identification, rows of trees were established in each block, labelled alphabetically starting with A in the east. Trees were then numbered sequentially along each row, starting from the north of each block.

A stem map was then created by uploading one of the ULS-derived canopy height models (CHMs – see section 3: *CHM generation*), and then manually annotating the trees, labelling them according to the field data. The stem map was then verified by assessing the associated aerial imagery of the stand to confirm tree locations.

2.3. Remote sensing capture methods

Three UAV laser scanning systems were evaluated: DJI Zenmuse L1 (DJIL1) mounted on a DJI Matrice 300 RTK UAV (Figure 3b), DJI Zenmuse L2 (DJIL2) mounted on a DJI Matrice 350 RTK UAV (Figure 3c), and the RIEGL MiniVUX-1 UAV mounted on a DJI Matrice 600 UAV (Figure 3a). The DJIL1 and DJIL2 flights were conducted using DJI Pilot 2 flight control software, while the MiniVUX flight was carried out using UgCS.

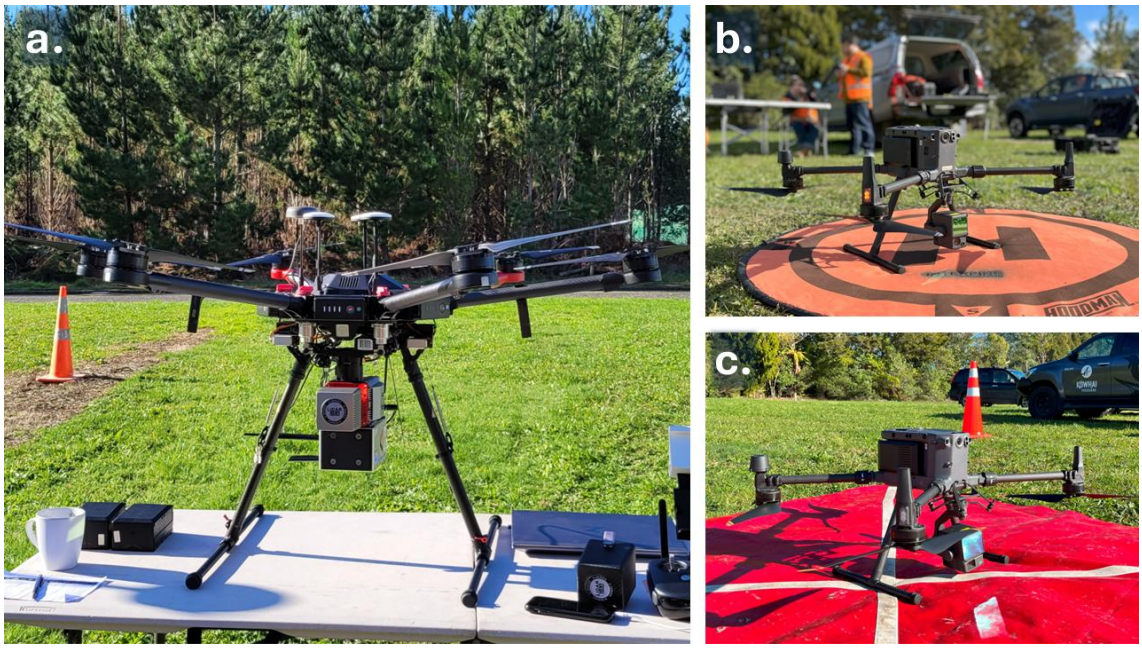

Figure 3. ULS sensors and respective platforms used in the trial: a. MiniVUX with DJI M600; b. DJIL1 on M300; c. DJIL2 on M350.

Prior to the flights, ground control points (GCPs) were established at each corner of the site and in the centre to provide accurate georeferencing for the ULS point clouds. To ensure the accuracy and consistency of the RTK base station location, a point was surveyed in the nursery near the take-off location using an Emlid Reach RS2, which has horizontal and vertical accuracies of 1 cm and 2 cm, respectively. This location was then entered into DJI RTK base station prior to every capture.

Flight parameters were kept consistent across sensors where possible, with all systems flown in repetitive scan mode and following a standard grid flight pattern. In total, 144 combinations of flight parameters, sensor configurations and stand conditions were tested. Flight parameters included two flight speeds, three flight line overlap combinations, two sensor types (with a third used as ground truth), two altitudes, two scan rates for the DJIL1 (DJIL2 has a single scan rate), and two settings for the number of returns. These flight parameters were then repeated across two stand condition treatments (understory/no understory), and across three stockings. A full list of all flight parameter combinations is provided in Table 1.

Forest Growers Research Ltd, PO Box 1127, Rotorua. Ph: 07 921 1883 Email: forestgrowersresearch@fgr.nz Web: www.fgr.nz

Table 1. Flight parameters tested in this study.

Flight parameter	Unit	Description	Settings tested
Flight speed	m/s	The forward velocity of the UAV during flight, which influences point density and coverage efficiency.	5, 10
Overlap	%	The proportion of overlap between adjacent flight lines; higher overlap increases point density and reduces gaps.	70, 80, 90
Number of returns	n	The number of laser returns recorded per pulse (e.g., first, last, multiple), influences the ability to capture both canopy and understory structure. “All” returns indicates the maximum number supported by each sensor: up to 5 returns for the MiniVUX and DJIL2 and 3 returns for DJIL1.	All, first only
Scanner	NA	The specific LiDAR sensor used (e.g., DJIL1, DJIL2, MiniVUX), each with different capabilities and accuracies.	DJIL1, DJIL2, MiniVUX
Scan rate	kHz	The frequency of laser pulses, i.e. the number of laser pulses emitted by the scanner per second.	Max (160) and min (80) for L1; Sole (240) for L2
Altitude	m AGL	The flying height above ground level; higher altitudes increase coverage area but reduces point density. Two altitudes were trialled: Scion's standard operating height (60 m), and the legal maximum for Civil Aviation Authority (CAA) Part 101 operations in AoNZ (120 m).	60 and 120
Understory	NA	Indicates whether felled material or natural vegetation was present beneath the canopy, which can influence detection of ground and lower stem points.	Y / N
Stocking	stems/ha	The number of trees per hectare; higher stocking increases canopy closure and competition, affecting visibility of individual stems in the point cloud.	833, 1111, 1667

Flights at 60 m altitude were conducted over a single area of interest (AOI), while a larger AOI was required for 120 m flights to ensure a sufficient margin outside the block edges and to allow the UAV to reach the desired speed before entering the stand. Figure 4 shows the flight path for a 120 m altitude flight with 70% side overlap, highlighting the extended buffer zone around the block.

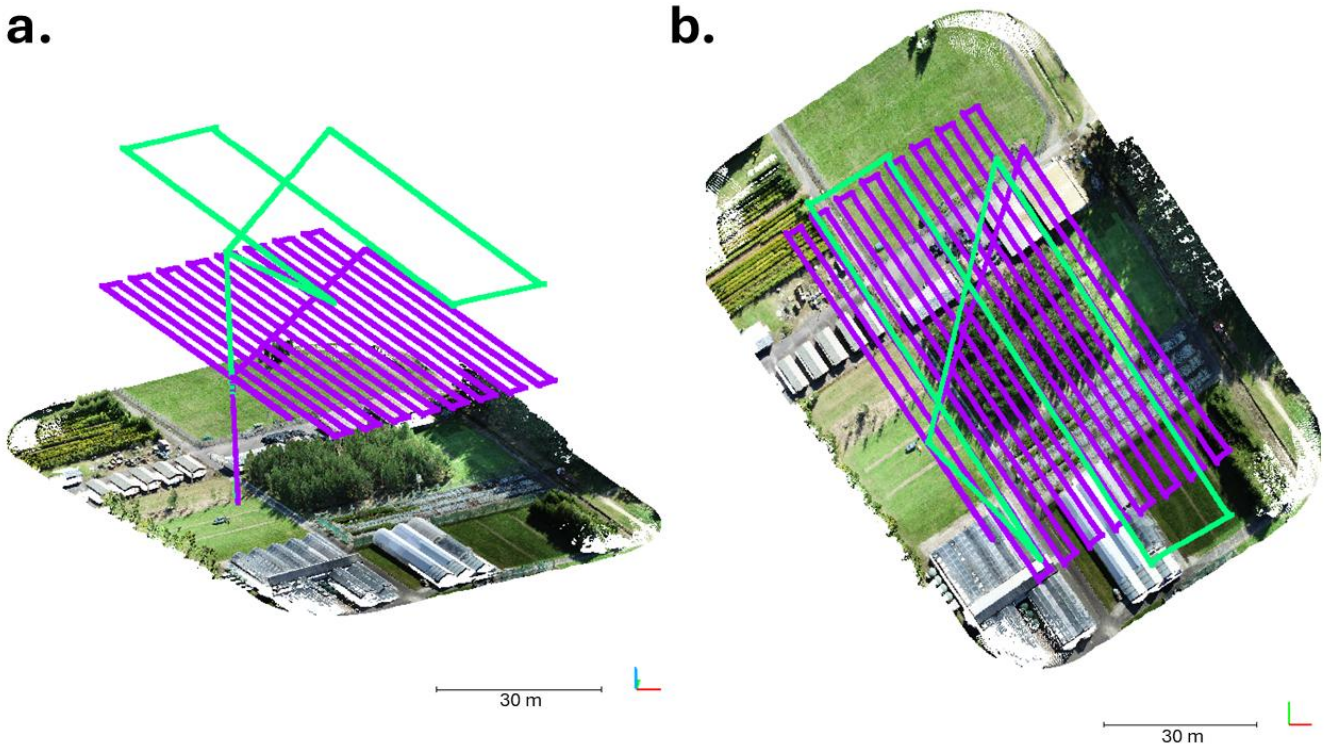

Figure 4. Variation in flight altitude and overlap: a. Side-on view, highlighting that flights were conducted at two different altitudes – 60 m (purple) and 120 m (green). b. Top-down view, highlighting that flights were also conducted at a range of overlaps – the extremes are indicated here with the 60 m AGL flight at 90% overlap, and 120 m AGL flight at 70% overlap between flight lines. Flightlines were extended beyond stand boundaries, ensuring a consistent speed over the area of interest and adequate coverage of the trees from all angles.

2.4. Processing

Raw data from the DJIL1 and DJIL2 sensors were processed into point clouds using DJI Terra, while MiniVUX data were processed into point clouds using ScanLook Point Cloud Export (ScanLook PC). All point cloud datasets were subsequently cropped using the lidR package in R (R Core Team, 2022; Roussel, et al., 2020) to isolate the trial area. Points captured during turns or taxi lines (e.g. take-off to first line), and repositioning were removed in R by combining the GNSS tracklog of the craft from the UAV flight logs with the point cloud data and filtering any flight lines that were not in-line with the main flight lines.

Pre-processing of the point clouds was conducted using LAStools (Isenburg, 2019), in which each point cloud was denoised, ground-classified, and both digital terrain models (DTMs) and CHMs were generated with a 1 m and 0.25 m resolution, respectively. Outputs from the pre-processing steps can be seen in Figure 5. For a full methodology detailing the processing steps, please refer to (Hartley, et al., 2025).

Forest Growers Research Ltd, PO Box 1127, Rotorua. Ph: 07 921 1883 Email: forestgrowersresearch@fgr.nz Web: www.fgr.nz

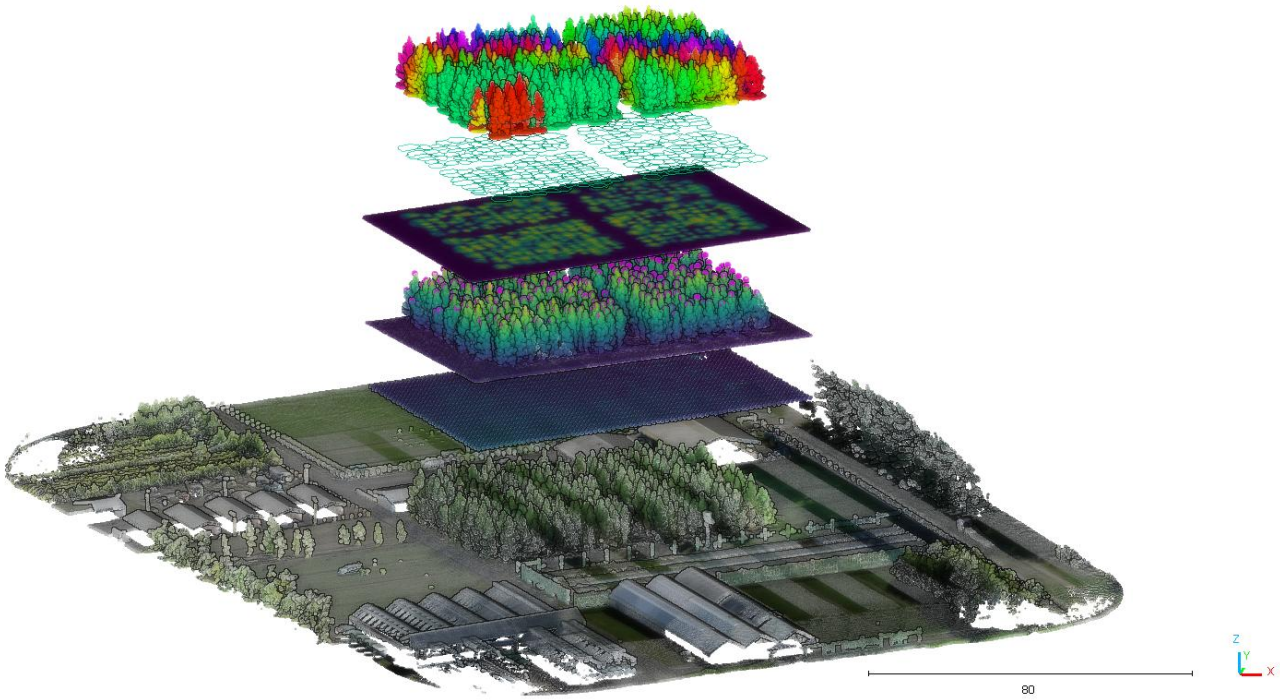

Figure 5. A 3D visualisation of the spatial layers derived from the pre-processing steps. From bottom: Raw colourised point cloud, DTM, cropped and height normalised point cloud with detected tree peaks (pink points), CHM, delineated crowns, and individual tree segments that are coloured according to their successive tree ID.

2.5. Individual tree detection and crown delineation

Individual tree detection (ITD) was carried out on the thinned point clouds using a local maxima filtering approach implemented in lidR. A stem map was manually digitised from the CHM and verified against field notes and UAV images to provide a reference dataset. Detected tree peaks from ULS were then compared against the stem map, with each detection classified as a true positive (TP), false positive (FP), or false negative (FN). An illustration of this matching process is provided in Figure 6.

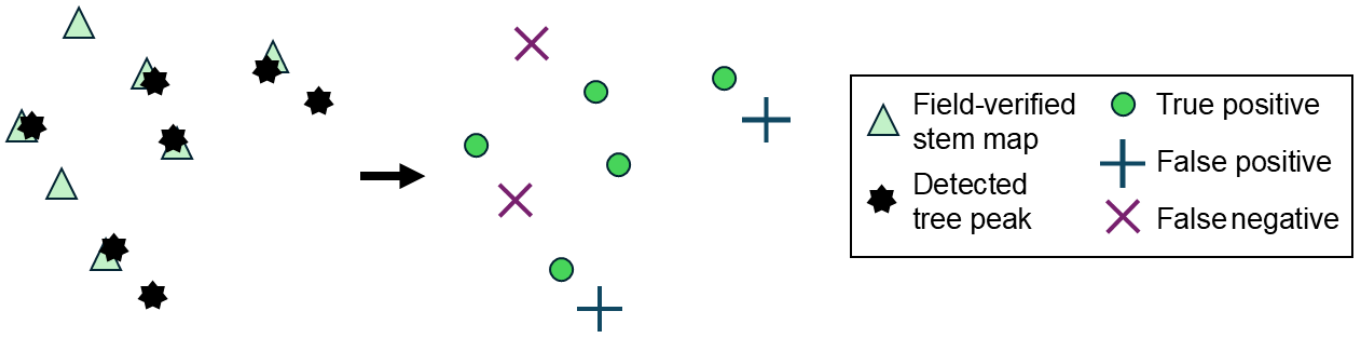

Figure 6. Individual tree detection methodology: Illustration of stem map matching step, where detected tree peaks (black stars) are sorted into true positives (green circles) and false positives (blue crosses), and any trees not detected are labelled as false negatives (purple crosses).

To ensure that the quality of the point clouds was being compared, and not biased by detection accuracy, crown delineation was conducted on each point cloud using the verified stem map. Crown delineation was conducted in R using a marker-controlled watershed segmentation algorithm applied to the CHM, implemented in the ForestTools package (Plowright, et al., 2021). The individual tree crown polygons were then used to segment the point clouds into individual tree segments, from which tree-level metrics could be extracted (Figure 5).

Forest Growers Research Ltd, PO Box 1127, Rotorua. Ph: 07 921 1883 Email: forestgrowersresearch@fgr.nz Web: www.fgr.nz

2.6. Individual tree metrics

To understand how well ULS can measure tree attributes, a range of individual tree metrics was calculated. These metrics describe different structural attributes, such as tree height, crown size, and the distribution of the foliage. Together, they give a complete representation of both the vertical and horizontal structure of each tree.

Metrics were calculated from the point cloud of each detected tree using specialist software in R. Basic measurements, such as tree height, laser return intensity, and crown density, were generated with the lidR package. To capture crown shape and volume, each tree point cloud was wrapped in a "convex hull" (a 3D outline that encloses the tree), allowing estimates of crown area, surface area, and volume.

For practical comparison with field data, maximum tree height (zmax) was used as the key height measure. A more detailed list of all the metrics tested can be found in Watt et al. (2024), but for this study, they can be grouped into four categories:

I. Height metrics – describing maximum and average tree height;
II. Laser intensity metrics – showing how strongly the laser reflects from different parts of the tree;
III. Crown density metrics – indicating how dense the canopy is;
IV. Crown shape metrics – estimating crown area, surface area, and volume using the convex hull method.

The processing, ITD, crown delineation and metric derivation pipeline for this paper has also been compiled into a single R package to enable industry users to carry out these steps efficiently. Please see https://github.com/ScionResearch/treenotypR.

2.7. Data analysis

Individual tree metrics were compared against field measurements to evaluate the influence of flight parameters and site conditions on ULS outputs. The following statistical analyses were conducted in R to quantify these effects:

When evaluating how accurately tree peaks could be detected from each of the different flight parameter combinations, a few simple measures were used. First, true positives (TP; trees correctly detected where a tree actually exists), false positives (FP; detections where no real tree is present), and false negatives (FN; real trees that were missed) were calculated by comparing the detected peaks with the stem map. From these, the overall performance was described using three metrics: precision indicates how many of the detected trees were real (i.e. how often the system is "right" when it says a tree is there), recall indicates how many of the real trees were actually found, and the F1 score provides a balanced measure of performance by combining precision and recall into a single metric. The equations for the calculation of these metrics are as follows:

$$\textbf{Precision} = \frac{\mathrm{TP}}{\mathrm{TP} + \mathrm{FP}}$$

$$\textbf{Recall} = \frac{\mathrm{TP}}{\mathrm{TP} + \mathrm{FN}}$$

$$\textbf{F1} = 2 \times \frac{\mathrm{recall} \times \mathrm{precision}}{\mathrm{recall} + \mathrm{precision}}$$

When comparing the accuracy of the derived CHMs and DTMs to the ground truth (the survey-grade MiniVUX-derived layers with no understory), the root mean squared difference (RMSD) was calculated. This statistic provides a single number that summarises how close, on average, the UAV-derived layers are to the reference layers. Small RMSD values mean the surfaces align closely with the ground truth, while larger values indicate greater differences.

The RMSD is calculated as:

$$\textbf{RMSD} = \sqrt{\frac{\sum_{i=1}^{n}(\hat{y}_i - y_i)^2}{n}}$$

where $\hat{y}_i$ are the values derived by the various parameter-test flights, y_i are the reference values from the MiniVUX, and *n* is the number of comparison points.

To assess how well the UAV measurements matched the field data, we compared two key attributes: tree height and DBH. For tree height, we looked at both precision (how consistently similar the UAV measurements were to one another) and accuracy (how close they were to the field-measured values).

For DBH, which was predicted from UAV-derived metrics for 2D crown area (based on CHM) and 3D crown area (based on fitting a convex hull to the individual tree point cloud), performance was evaluated using two common measures. The coefficient of determination (R^2) shows how well the UAV predictions track the field measurements, with values closer to 1 meaning the UAV predictions follow the same trend as the measured DBH. The root mean square error (RMSE) expresses the typical size of the prediction error in the same units as DBH (cm), making it easy to see, on average, how far the estimates were from the field-measured values. Lower RMSE values mean more accurate predictions. R^2 and RMSE were calculated as follows:

$$\mathbf{R^2} = \frac{\sum_i (\hat{y}_i - \bar{y})^2}{\sum_i (y_i - \bar{y})^2}$$

RMSE and RMSD refer to the same statistical measure, but in the context of raster comparisons, such as DTMs, RMSD is the more commonly used term. Consequently, RMSE and RMSD use the same calculation, but for both R^2 and RMSE in this scenario, $\hat{y}_i$ represent the values derived by the various parameter-test flights, y_i represent the reference values from the field data. As RMSE comparisons can be more meaningful when represented as a percentage, the relative RMSE (RMSE%) was calculated by expressing the RMSE as a percentage of the average observed values as follows:

$$\mathbf{RMSE}\% = \left(\frac{\mathrm{RMSE}}{\bar{y}}\right) \times 100$$

To compare the different flight parameter combinations, the performance of the resulting point clouds was assessed for their ability to derive five important forestry measurements: tree detection, canopy height, terrain, tree height, and DBH. To do this, accuracy metrics were derived for a metric derived from the point clouds to the ground truth (see Table 2).

Table 2. Accuracy metrics for each forestry measurement, alongside the ground truth used to assess accuracy.

Measurement	Ground truth	Metric
Tree detection	Stem map	F1 (detection accuracy)
Canopy height	MiniVUX CHM	CHM RMSD
Terrain	MiniVUX DTM	DTM RMSD
Tree height	Field height	RMSE of heights
DBH	Field DBH	R^2 3D crown area vs field DBH
		R^2 2D crown area vs field DBH

We analysed LiDAR performance metrics across flight-parameter settings (sensor, overlap percentage, scan rate, all or first returns, altitude and speed) and site conditions (stand stocking, presence of understorey).

Three model scopes were fit per metric using linear models with Type-III ANOVA (sum contrasts):

(i) Overall: using all the trees in the AOI;
(ii) Per-stocking: separate models for each block with distinct stocking;

Forest Growers Research Ltd, PO Box 1127, Rotorua. Ph: 07 921 1883 Email: forestgrowersresearch@fgr.nz Web: www.fgr.nz

(iii) Pooled: one model with stocking as a factor, and interactions between stocking, flight parameters and covariates.

For each model we reported measures of the effect size (η^2 and ω^2) to show how much each factor influenced the results. As a cross-check, we ran a random forest model and recorded the importance of each variable using a permutation approach.

For flight-parameter selection, we first removed constants that would cause duplication or conflicts. We then tested all combinations of flight settings and aggregated the results per combination. These were then ranked depending on the goal of the metric: higher is better for F1 and R^2, lower is better for RMSE/RMSD. This produced:

- Per-metric summaries (showing the best settings combinations, ranked),
- Cross-metric comparison tables (overall, by-stocking, and combined),
- Effect and importance plots to highlight which parameters matter most.

3. Results and Discussion

In total, this study assessed 144 flight parameter and site condition combinations for the DJI sensors. When evaluated across five performance metrics, this created a total of 720 ranked variables for optimisation. While we have conducted a robust statistical analysis of these data, this report focuses on general trends to inform industry best practice. A more detailed statistical analysis will be provided in a peer-reviewed analytical journal article.

The results and discussion are therefore combined and structured as follows: the impact of flight parameters on point density and flight times, which are important operational considerations for efficiency. Next, the overall performance across the five performance metrics (tree detection, CHM, DTM, height and DBH accuracies), followed by a more detailed appraisal of how flight parameters affect each metric individually. The impact of key stand conditions (understory and stocking) is explored. Finally, although outside the main scope of this project, we include insights from a small exploratory trial of the DJIL2 in non-repetitive scan mode. While not conclusive, these results should provide useful preliminary insights into the potential of this mode.

Flight times

Key takeaway: Overlap percentage has the strongest effect on flight duration, lowering overlap greatly improves efficiency, while speed and altitude have smaller impacts.

One key factor that foresters are interested in when planning UAV forestry operations is how long it will take. Efficiency gains can be made by flying higher, reducing overlap or increasing speed; however, there may be trade-offs with data quality, which we will discuss later. The minimum and maximum flight times for flying this 0.5 ha stand to achieve the required coverage were 5m29s and 20m56s, respectively. As these times cannot be readily scaled to larger blocks due to taxi times (from take-off to start position and from end of flight to take-off) and overflights took up a large part of the flight paths, the flight times were normalised as a percentage of the longest flight time. This enables more meaningful comparisons. The normalised flight times for a group of flights that comprises all of the combinations of flight speed, overlap and altitude assessed in this study can be seen in Figure 7.

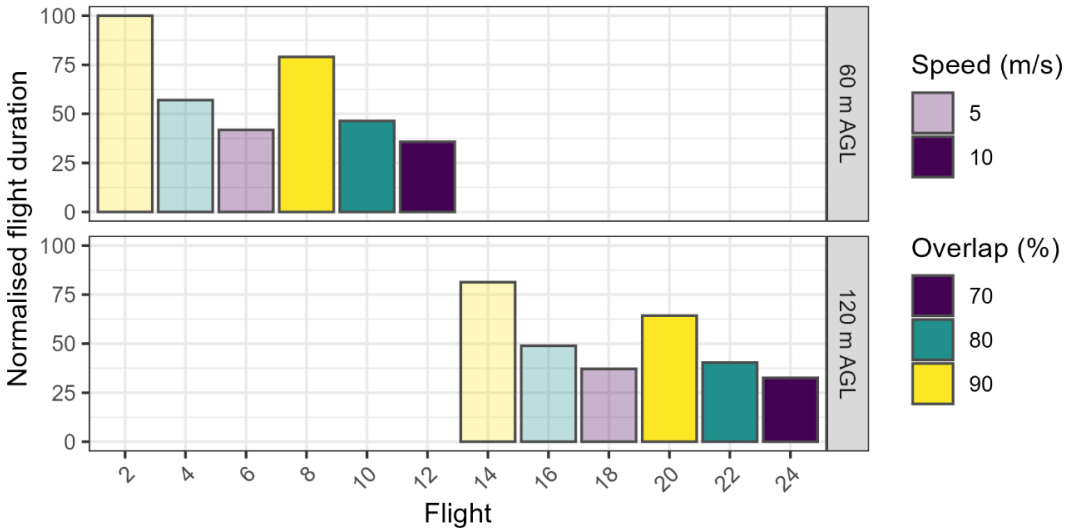

Figure 7. Flight time efficiency: Bar plots showing flight duration (normalised as a percentage of the longest flight time) for a selection of the DJIL1 flight plans, representing the entire range of flight times assessed at different altitudes. Bars are coloured according to overlap with the bar transparency levels reflecting the different flight speeds (10 m/s = solid, 5 m/s = opaque).

The least efficient flight occurred, as expected, at the lowest altitude and speed combined with the highest overlap. In contrast, the most efficient flight time, only 32% of the least efficient flight, was achieved under the opposite conditions: the highest altitude and speed with the lowest overlap.

The parameter that has the most significant impact on flight time is overlap, which has a mean flight time difference between the flight parameter combinations of ~44%, compared to mean differences of ~11% and ~9% for speed and altitude (Table 3).

Table 3. Impact of three key parameters on flight time, expressed as the mean and standard deviation (SD) of the difference between normalised flight times.

Parameter	Mean difference (%)	SD difference (%)
Altitude	9.2	6.1
Speed	11.3	6.5
Overlap	44.3	10.9

These results indicate that if efficiency is prioritised over data quality, then reducing overlap to 70% will provide the biggest time saving. In the next sections, we will assess the impact of different parameters on accuracy and determine how much of an impact this reduction in overlap has on the quality of the data and the derived results.

Point Density

Key takeaway: Point density increases most when overlap is high, altitude is low, and speed is reduced, but foresters must balance the benefits of greater accuracy with the cost of larger data storage requirements.

Along with flight times, foresters are also concerned with data size. With lidar data, point density is equivalent to data size as the more points there are in a cloud, the more disk space they require. Point density is driven by four key parameters – overlap, speed, altitude and scan rate. As can be seen in Figure 8, the greatest point density was attained with the flights at the highest overlap, lowest altitude, and speed, with the DJIL2 scanner (which has a much higher scan rate than DJIL1). Data density is an important consideration, but as with flight time efficiency, the trade-off of data storage requirements must be balanced against the gains in accuracy that can be achieved at different parameter combinations. The information within this report can be used by foresters to help make that assessment.

Forest Growers Research Ltd, PO Box 1127, Rotorua. Ph: 07 921 1883 Email: forestgrowersresearch@fgr.nz Web: www.fgr.nz

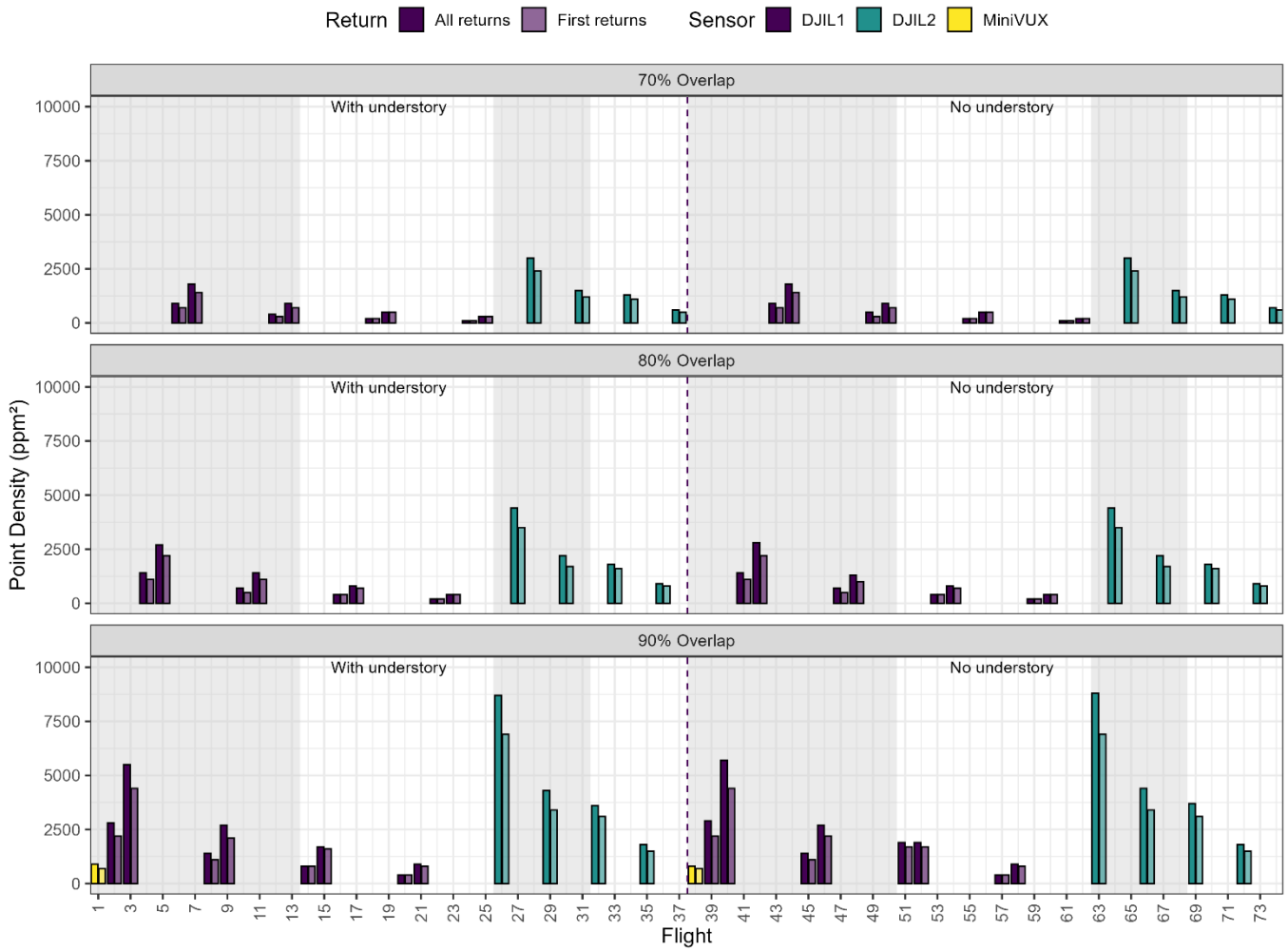

Figure 8. Point density per flight. The three panels show flights conducted at different overlaps, from top to bottom: 70%, 80%, 90%. Bars show point density (ppm²) for each flight, coloured by sensor. Darker bars represent analysis of all returns; lighter bars represent first returns only. Grey-shaded panels indicate flights at 60 m AGL; white panels indicate 120 m AGL. Flights to the left of the dashed line were conducted with understory present; flights to the right were conducted with understory removed. Within each altitude-shaded section of the plot, there are two clusters of flights – the first (from left to right) represents flights at 5 m/s, and the second is flights at 10 m/s.

Overall performance

From the analysis of the point clouds from the different flight parameter combinations, some clear trends emerged. Results for the best overall parameter combinations for each metric can be found in Table 4. The trends will be discussed further in this section and the top findings will be contrasted with the top five ranked results to identify any combinations that may be more robust.

Key takeaway: DJIL2 outperformed DJIL1 overall, thanks to its narrower beam divergence, higher precision, and denser point clouds. Best results came from low altitude (60 m AGL), high overlap (80–90%), high scan rates, and using all returns. Flight speed mattered less, though lower speed favoured the tree height metrics. Multiple returns were essential for accurate structure and terrain, while first returns sufficed only for tree detection.

Forest Growers Research Ltd, PO Box 1127, Rotorua. Ph: 07 921 1883 Email: forestgrowersresearch@fgr.nz Web: www.fgr.nz

Table 4. Overall best parameter combinations for each measurement. When multiple combinations tied for first place, all of them were recorded as top-ranked. The parameters are also ranked in terms of their influence on the measurement.

Measurement	Performance Metric	Best parameter combination						FlightIDs	Top 6 most influential parameters
		Sensor	Speed (m/s)	Overlap (%)	Scan rate	Returns	Altitude AGL (m)		
Tree detection	F1 (ITD accuracy)	DJIL1	10	70	160	All	60	25, 99	sensor > speed > overlap % > scan rate > returns > altitude
		DJIL2	5	80	240	All	60	127, 53	sensor > speed > overlap % > scan rate > returns > altitude
Canopy height	CHM RMSD	DJIL2	5	80	240	All	60	127, 53	speed > sensor > altitude > scan rate > overlap % > returns
Terrain	DTM RMSD	DJIL2	10	90	240	All	60	131, 57	sensor > overlap % > speed > altitude > returns > scan rate
Tree height	RMSE of heights	DJIL2	5	90	240	All	60	131, 57	overlap % > speed > scan rate > altitude > sensor > returns
DBH	R^2 3D crown area vs field DBH	DJIL2	10	80	240	All	60	133, 59	overlap % > scan rate > returns > sensor > speed > altitude
		DJIL2	10	90	240	All	60	131, 57	overlap % > scan rate > returns > sensor > speed > altitude
		DJIL2	5	80	240	All	60	127, 53	overlap % > scan rate > returns > sensor > speed > altitude
	R^2 2D crown area vs field DBH	DJIL2	10	70	240	All	60	135, 61	overlap % > sensor > speed > scan rate > altitude > returns
		DJIL2	10	80	240	All	60	133, 59	overlap % > sensor > speed > scan rate > altitude > returns

Forest Growers Research Ltd, PO Box 1127, Rotorua. Ph: 07 921 1883 Email: forestgrowersresearch@fgr.nz Web: www.fgr.nz

Sensor: The obvious result is that the DJIL2 generally outperformed the DJIL1 in all aspects, except for tree detection, where the best-performing DJIL1 parameter combination was tied with the best-performing DJIL2 combination (Table 4). When looking at the top 5 parameter combinations for each accuracy metric, it is clear that DJIL2 outperformed the DJIL1 across all of them (Figure 9). However, DJIL1 appeared in the top 5 flight parameter combinations as often as DJIL2 for CHM accuracy and was actually found more often in the top 5 parameter combinations for tree detection (Figure 9). The better performance of the DJIL2 was not unexpected as it has a significantly lower beam divergence, resulting in a smaller laser footprint that enables better canopy penetration and more accurate resolving of canopy. The DJIL2 boasts better range precision, which directly improves vertical accuracy (i.e. tree height) and DTM quality, and an increased number of returns, making it better able to register intermediate and last returns, enabling better DTM creation and structural characterisation. Other improvements include a superior IMU and GNSS for improved locational accuracy (less noise in point clouds), and a wider field of view (resulting in less edge noise and better crown delineation).

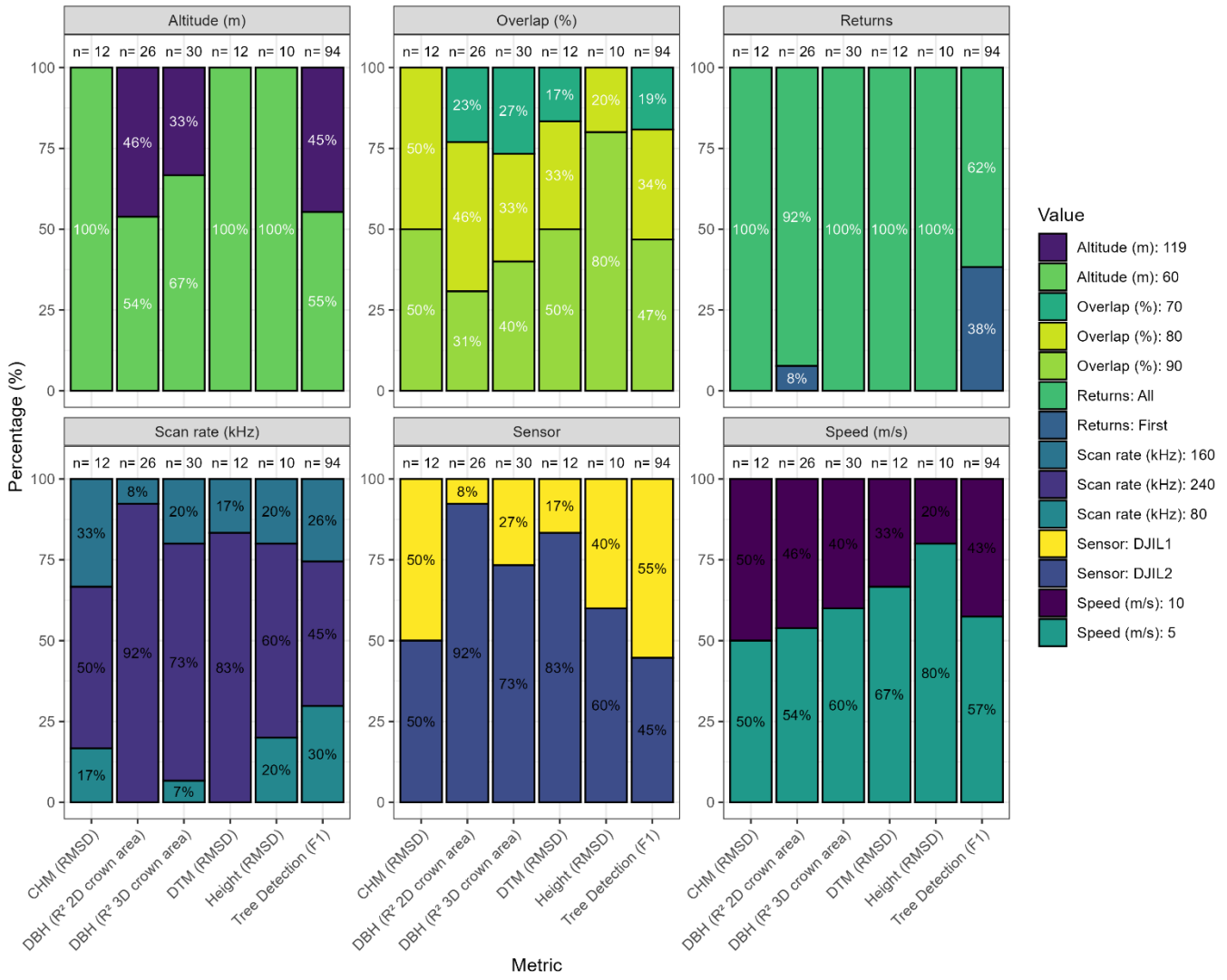

Figure 9. Relative frequency of parameter settings appearing in the top 5 ranked combinations for each evaluation metric. Bars show the percentage of appearances of each parameter value (e.g., sensor type, flight speed, overlap) among the top 5 combinations, with ties included. Black outlines indicate stacked contributions of different parameter values within each category. As ties can inflate the number of appearances, "n" value at the top of each column represents the total number of flights included in the top 5 parameter combinations – i.e. the higher the number, the more tied rankings.

Flight speed: Lower speeds (5 m/s) performed best for height-related metrics (canopy height, tree height) and tied with 10 m/s for tree detection and DBH prediction from 3D crown area (which uses height), while 10 m/s was optimal for terrain, and DBH prediction from 2D crown area. When looking at the occurrences of the two speeds in the top 5 parameter combinations, the split is pretty even; however, 5 m/s is clearly more important for height, and interestingly, 10 m/s occurs more frequently than 5 m/s. This indicates that although 5 m/s gives better results, 10 m/s could

Forest Growers Research Ltd, PO Box 1127, Rotorua. Ph: 07 921 1883 Email: forestgrowersresearch@fgr.nz Web: www.fgr.nz

potentially offer results with comparable accuracy. The even split also indicated that speed is less of a critical parameter than altitude or returns, with both speeds being able to achieve near-optimal results.

Altitude: The lower altitude of 60 m AGL was optimal across the board for all measurements (Table 4). From the analysis of the top 5 parameter combinations, it is clear that the lower altitude is crucial for height-based metrics (CHM, DTM and tree height), but less so for DBH and tree detection. These results make sense because at a lower altitude, point density will increase as the laser "fan" is more focused, and with it canopy penetration will increase. It is also more likely that the tips of the trees will be detected when the laser returns are more closely clustered. Flying low is not always practical for forestry operations (for example pre-harvest inventory). Encouragingly, the results show that higher-altitude flights appeared almost as frequently in the top 5 combinations for tree detection and DBH prediction, indicating that practical constraints can be accommodated without major losses.

Returns: "All returns" was also consistently optimal, in both the top performing and top 5 parameter combinations (Table 4, Figure 9), highlighting the value of capturing full return information. More returns are crucial to capture information about the below-canopy vegetation and terrain, with the intermediate returns providing better information on tree structure, enabling better DTM creation and structural characterisation. Interestingly, nearly ~40% of the top 5 parameter combinations for tree detection were from first returns only. The higher number of flights (n = 94) included in the top 5 means that there were significant numbers of ties, which indicates that the use of first or all returns is less crucial for tree detections (Figure 9). This result is self-explanatory: the apex of the tree is identified by the local maxima algorithm, and since the apex is the highest point, it is easily captured by the first returns of the laser.

Scan rate: The highest scan rate (240 kHz) was best for all metrics, except for stocking, where a lower rate (160 kHz – the highest setting for the DJIL1) was tied for first place (Table 4). Looking at the top 5 offers some additional insights here. 240 kHz is the sole setting for DJIL2 and, for DBH estimation and DTM accuracy, DJIL2 was clearly the dominant sensor appearing in the top 5 combinations. This point can be explained by the denser point clouds created at higher scan rates, which enable fine structural characterisation and improve ground point detection. For the other metrics, when looking at the split of the residual scan rates, the higher rate of DJIL1(160 kHz) was approximately equal to the lower scan rate (80 kHz), aside from CHM accuracy, where the higher rate was more prevalent. DJIL1 scan rates combined were also equally represented in the top 5 for CHM and ITD accuracy as the DJIL2 rate of 240 kHz. CHM and ITD rely less on maximum density than on canopy coverage, so DJIL1 still performed competitively for these metrics.

Overlap: Lastly, higher overlaps (80–90%) were beneficial for most performance metrics, except tree detection and DBH predicted from 2D crown area, which both optimised equally at 70% and 80%, respectively (Table 4). When looking at the top 5 parameter combinations however, we can see that 90% overlap is dominant for height and DBH estimates from 3D crown area (where vertical accuracy is of paramount importance), 80% is equally as frequent as 90% overlap for CHM accuracy, and 70% is the least frequent for all metrics, except CHM and height, where it is not in the top 5. This demonstrates that, overall, the top results can be achieved by using a high overlap of 90%, but 80% is likely a good alternative for those wishing to increase flight time efficiency (Figure 7).

Tree detection accuracy

Key takeaway: Tree detection accuracy is mainly driven by overlap. DJIL1 is highly sensitive to overlap, while DJIL2 is more stable. Using all returns greatly improves precision, especially at lower overlaps, making multiple returns essential for reliable detection.

When assessing the tree detection accuracy, the best performing sensor, according to F1 score (the harmonic mean of precision and recall) was DJIL1 at a speed of 10 m/s with a 70% overlap, at the scanner's maximum scan rate (160 kHz), using all returns and at an altitude of 60 m AGL (Table 4). This suggests that a slightly coarser acquisition favours detection of tree stems/crowns. When looking at the precision and recall values of the flights; however, it is interesting to note that tree detection performance is driven largely by the overlap (Figure 10). The DJIL1 is much more impacted by overlap than DJIL2, as can be seen by the grouping of the flights across the different overlap combinations (Figure 10). The number of returns used also interacted with the overlap. For example, in the DJIL1, the precision of flights with first returns only was significantly lower at 70% overlap than flights with all returns, i.e. less of the detected trees were actually trees. However, this trend was less pronounced at 90% overlap, which demonstrates that the use of multiple returns is crucial for low overlap flights. The trends were not as apparent with DJIL2, where precision and recall were more uniform across the different overlaps. The lowest precision attained by DJIL2 was, however, still with the first returns only flights, supporting the contention that multiple returns are beneficial for peak detection.

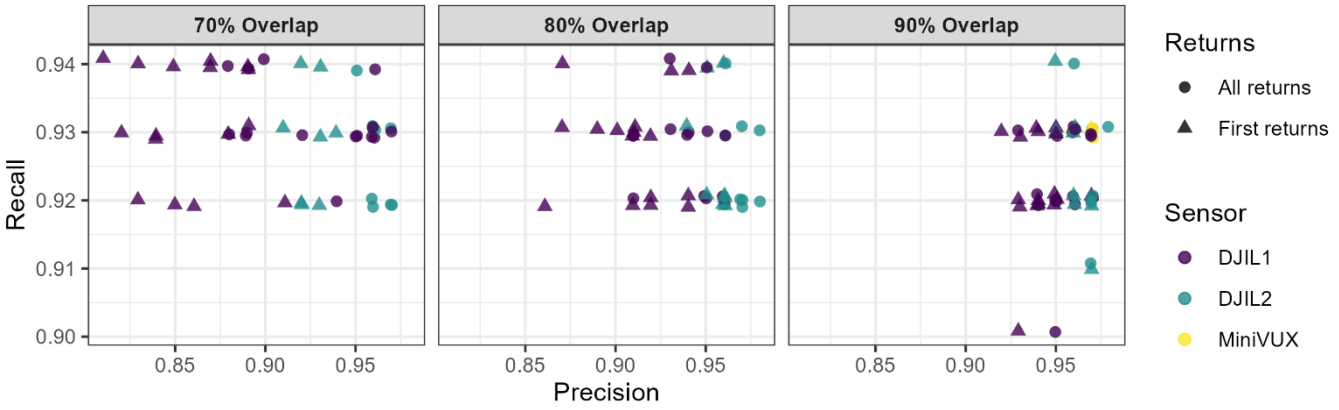

Figure 10. Precision and recall plots showing detection accuracy metrics for flights at three different overlaps. Points are coloured by sensor and shaped according to the number of returns.

CHM generation

Key takeaway: CHM accuracy is more sensitive to flight settings than DTMs or tree heights, with lower, slower flights and higher point densities providing the most precise canopy models, and DJIL2 consistently outperformed DJIL1, especially when site has complex understory conditions.

Some clear trends were observed when comparing the accuracy of the CHMs created from the different flight parameter combinations. Overall, the best results were achieved with DJIL2 sensor flown at 5 m/s, with 80% overlap, standard 240 kHz scan rate, using all returns, and at 60 m AGL (Table 4). This suggests that canopy measurement accuracy benefits from increased point density.

When examining RMSD across flights, several trends are apparent (Figure 11). First, flight speed has sensor-specific effects. DJIL1 consistently shows higher RMSE than DJIL2, regardless of speed or altitude, underscoring sensor choice as the dominant factor, whilst parameter selection can be used to fine-tune the performance of the sensor. DJIL2 not only had better performance but was more stable across flight parameter combinations compared to the DJIL1, making it a more robust sensor choice. For DJIL1, slow flights tended to decrease RMSD, while for DJIL2, speed had less influence. The effect also diminished at higher altitudes, reinforcing the fact that flying lower provides greater gains than simply adjusting speed alone.

Second, the difference between using only first returns and all returns is more pronounced at lower altitude. This improvement is concentrated in the shaded (low altitude) panels of Figure 11. This indicates that multiple returns provide significant accuracy gains when flying low, whereas at higher altitudes the advantage diminished. Results also show that higher flight altitudes generally produced poorer accuracy. The survey-grade MiniVUX data was used as the ground truth for CHM accuracy. It is interesting to note that there is minimal difference between datasets captured with and without understory; however, the impact of using just first returns is still present.

A subtler trend was also observed within each cluster of flights. For both DJIL1 (six flight pairs per cluster in Figure 11) and DJIL2 (three flight pairs per cluster in Figure 11), flight pairs were ordered from higher overlap (90%) on the left to lower overlap (70%) on the right. Within these clusters, RMSD values tend to skew to the right, indicating that higher overlap reduces RMSD. While this effect is less pronounced than those of altitude, return type, or sensor choice, it nevertheless reinforces the role of point density in improving CHM accuracy.

Finally, the presence of understory has a stronger impact on accuracy in low-altitude flights, highlighting that non-tree vegetation structure interacts with flight parameters to influence CHM accuracy.

Forest Growers Research Ltd, PO Box 1127, Rotorua. Ph: 07 921 1883 Email: forestgrowersresearch@fgr.nz Web: www.fgr.nz

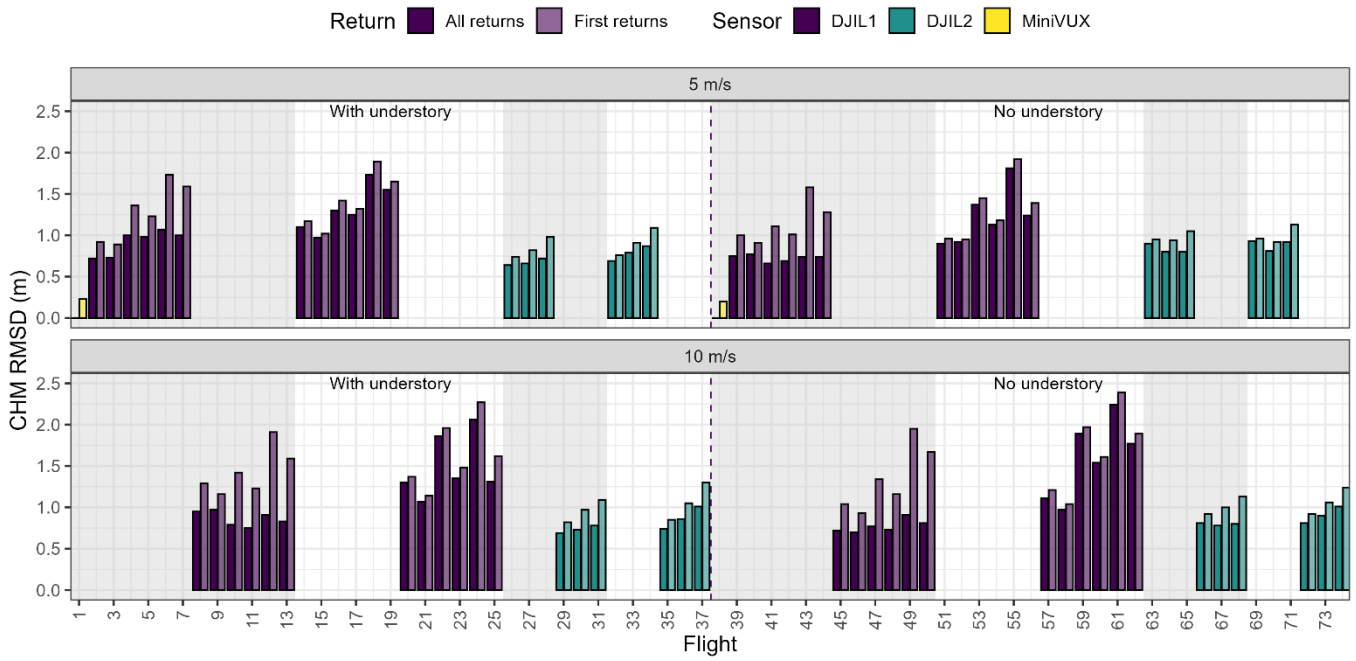

Figure 11. CHM accuracy per flight, where each bar represents a unique flight parameter combination. The top and bottom plots show flights conducted at 5 m/s and 10 m/s, respectively. Bars show the RMSD of the CHM for each flight, coloured by sensor. Darker bars represent analysis of all returns; lighter bars represent first returns only. Grey-shaded panels indicate flights at 60 m AGL; white panels indicate 120 m AGL. Flights to the left of the dashed line were conducted with understory present; flights to the right were conducted with understory removed. Within each cluster of flights, bars are ordered by overlap (90% on the left, 70% on the right). A slight increase in RMSD can be seen with reduced overlap.

DTM generation

Key takeaway: DTM accuracy is generally very high and less sensitive to flight parameters but capturing all returns at lower altitudes is essential for reliable ground detection, with DJIL2 delivering results close to a survey-grade ULS system at a fraction of the cost.

Results for DTM generation showed similar trends to CHM generation. The best results were achieved with DJIL2 sensor flown at 10 m/s, with 90% overlap, standard 240 kHz scan rate, using all returns, and at 60 m AGL (Table 4). This again suggests that terrain measurement accuracy benefits from increased point density. Overall, RMSD levels are lower for DTMs than CHMs, with most flights producing RMSD values well below 1 m, often <0.5 m, showing DTMs are generally more accurate and less sensitive to flight parameter variation than CHMs.

Again, a sensor effect was observed, with DJIL2 consistently producing lower RMSDs and less variability across flight parameters than DJIL1, mirroring the CHM results. DJIL1 exhibited higher RMSDs, especially under conditions with understory.

The difference between using all returns and only first returns is much more pronounced in DTMs than in CHMs. Using only first returns substantially increased RMSD (bars are visibly taller for “first returns”), highlighting the importance of capturing multiple returns for ground modelling. It is particularly notable that there was little change between the RMSDs of flights including first returns only between the understory and the no understory flights. This indicates that very few of the returns from the first returns datasets are actually able to penetrate vegetation to the ground surface when an understory is present.

In terms of altitude, the lower altitude flights consistently yielded lower RMSDs, as seen by the grey shaded (60 m AGL) vs. white (120 m AGL) zones in Figure 12. There is less of an accuracy penalty for higher altitude flights with DJIL2. Unlike CHMs, flight speed (5 vs. 10 m/s panels) appears to have a minimal impact on DTM RMSD, suggesting that point density from speed is less critical for ground detection compared to canopy mapping. Although the best flight that overall produced the lowest RMSD was conducted at 10 m/s, the general trend is for 5 m/s flights to be more accurate.

Forest Growers Research Ltd, PO Box 1127, Rotorua. Ph: 07 921 1883 Email: forestgrowersresearch@fgr.nz Web: www.fgr.nz

The dashed line split in Figure 12 shows a strong effect of understory: flights with understory present generally had higher RMSDs. This effect is particularly marked for DJIL1. DJIL2 seems to be more robust, but still shows some degradation when understory is present. It is also notable that DTMs derived from the DJIL2 are very close to the ground truth measurements taken by the survey-grade MiniVUX system, which was approximately tenfold the cost of the DJIL2. DJIL1 also produced very low RMSD at lower altitude with no understory, demonstrating that with appropriate parameter tuning, the system can still achieve high accuracy, given the right conditions.

As with the CHM figure (Figure 11), clusters of paired flights show that higher overlap (left of clusters) generally yielded lower RMSDs (Figure 12), particularly for first returns datasets. This effect is visible but subtle compared to return type, altitude, and understory.

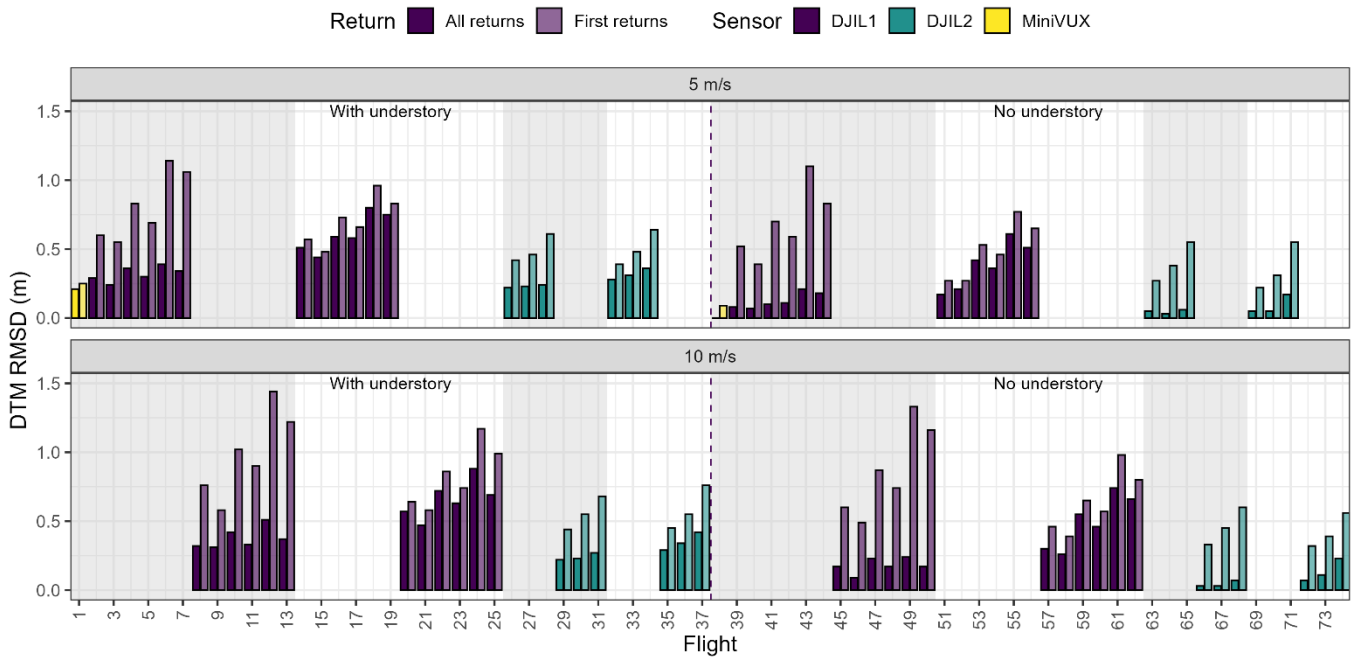

Figure 12. DTM accuracy per flight, where each bar represents a unique flight parameter combination. The top and bottom plots show flights conducted at 5 m/s and 10 m/s, respectively. Bars show the RMSD of the DTM for each flight, coloured by sensor. Darker bars represent analysis of all returns; lighter bars represent first returns only. Grey-shaded panels indicate flights at 60 m AGL; white panels indicate 120 m AGL. Flights to the left of the dashed line were conducted with understory present; flights to the right were conducted with understory removed. Within each cluster of flights, bars are ordered by overlap (90% on the left, 70% on the right). A slight increase in RMSD can be seen with reduced overlap.

Height measurements

Key takeaway: Accurate tree height measurement with ULS depends far more on flying lower and using all returns than on sensor choice or flight speed, with DJIL2 proving both robust and cost-effective compared to higher-end systems.

For height, DJIL2 again delivered the best result, achieved at 60 m AGL, flown at 5 m/s, with 90% overlap, the standard 240 kHz scan rate, and using all returns (Table 4). Height RMSEs fall between the RMSD values for DTMs and CHMs - generally higher than DTMs but lower than CHMs. This reflects the greater challenge of capturing canopy tops compared to terrain but less variability than full canopy models.

Altitude was the dominant parameter. The lower flights (60 m AGL/grey shaded zones of Figure 13) consistently produced lower RMSEs compared to higher flights (120 m).

The results show that using all returns improves accuracy over first returns across nearly all conditions. This trend is most notable for flights at low overlap and low altitude, suggesting that multiple returns are beneficial for accurately detecting tree peaks. This is particularly important when understory is present, since multiple returns increase canopy penetration and better capture treetops.

Forest Growers Research Ltd, PO Box 1127, Rotorua. Ph: 07 921 1883 Email: forestgrowersresearch@fgr.nz Web: www.fgr.nz

The highest overlap (90%) generally reduced RMSEs, although the effect is less pronounced than altitude or returns. Speed had less of an effect on accuracy, but there is a general trend for the 5 m/s flights to perform better than the 10 m/s within each cluster, especially for DJIL1 (Figure 13).

As with DTM and CHM accuracy, a sensor effect was evident, with DJIL2 consistently outperforming DJIL1, with lower RMSE and less variability. The MiniVUX matches field height most closely, but at a far higher cost, reinforcing the value of DJIL2 as a lower-cost alternative. Interestingly, within the no understory and understory collections of flights, DJIL1 consistently provided the closest match to the MiniVUX.

It is unusual that understory presence increased RMSE across all sensors and overlaps. This is counterintuitive as, even for flights only using single returns, there is an improvement in RMSE. This phenomenon is more likely due to bias in the field data than the influence of the understory on accuracy. Previous research has demonstrated that field-measured heights are often biased, tending to overestimate height due to difficulties in accurately identifying the tree base and top from distance (Larjavaara, et al., 2013; Wang, et al., 2019). Our results support this, as the tree heights from datasets with understory, which used a DTM to derive tree heights that we have demonstrated to have a higher RMSD (Figure 12), were closer to the field-measured heights. This is an important finding for industry, because the sector currently gauges the accuracy of lidar heights against field heights, whereas in reality it should be the other way around. The results also indicate that DJIL2 shows more robustness to different parameter combinations under understory than DJIL1 but still experiences some degradation.

Figure 13. Tree height accuracy per flight. The three panels show flights conducted at different overlaps, from top to bottom: 70%, 80%, 90%. Bars show tree height RMSE (m) for each flight, coloured by sensor. Darker bars represent analysis of all returns; lighter bars represent first returns only. Grey-shaded panels indicate flights at 60 m AGL; white panels indicate 120 m AGL. Flights to the left of the dashed line were conducted with understory present; flights to the right were conducted with understory removed. Within each altitude-shaded section of the plot, there are two clusters of flights – the first (from left to right) represents flights at 5 m/s, and the second is flights at 10 m/s.

Forest Growers Research Ltd, PO Box 1127, Rotorua. Ph: 07 921 1883 Email: forestgrowersresearch@fgr.nz Web: www.fgr.nz

DBH prediction

Key takeaway: DBH prediction using 3D crown area is consistently more accurate and robust than using 2D crown area, and with flight parameter tuning, can perform competitively compared to machine learning approaches applied in earlier studies, delivering R^2 values often >0.7. Sensor choice remains the dominant driver of accuracy (DJIL2 performs better than DJIL1), while overlap and altitude provide modest benefits, and return type/understory have minimal influence. Importantly, DBH prediction is relatively insensitive to variation in stand conditions, making it a stable metric for operational forestry applications.

Previous research has shown that by using machine learning, DBH can be predicted with moderate to strong accuracy with a mean R^2 = 0.71 (R^2 range = 0.33-0.90; (Watt, et al., 2025)). Results from the current study fall comfortably within the reported range in this previous study, even though a single predictor metric (crown area) was used as a predictor variable rather than machine learning approaches. Using only 2D crown area, DBH predictions were consistently moderate (R^2 = 0.40–0.69). When using 3D crown area, predictions were stronger again but more influenced by flight parameters, with a range of R^2 = 0.44-0.80). Overall, the best results were achieved with DJIL2 flying at 10 m/s, 80% overlap, standard 240 kHz scan rate, all returns and at 60 m AGL (Table 4). The following analysis uses 3D crown area as a predictor of DBH.

DJIL2 achieved higher R^2 than DJIL1 across most conditions, aligning with trends for CHM, DTM, and height accuracy. DJIL2 achieved comparable results with the survey-grade MiniVUX in predicting DBH (R^2 = 0.80 for both), again highlighting the strong relative performance of DJIL2.

Unlike for DTM and CHM accuracy, the difference between using all returns and first returns was minimal overall, particularly for DJIL2 and MiniVUX. For DJIL2, there was a notable difference in accuracy between first and all returns for flights with low overlap and high altitude combinations (Figure 14). This suggests DBH prediction from 3D crown area is less sensitive to return type. This is likely because crown area is derived from the canopy surface, rather than requiring penetration to ground or intermediate layers.

Higher overlaps (90%) yielded slightly higher R^2 compared with 70% or 80%, especially with DJIL1, but overall overlap has minimal impact on accuracy, apart from when only using first returns. DJIL2 remains largely consistent across all overlap combinations, suggesting this sensor is more robust and could be useful for improving time efficiencies. The trend for DJIL1 is subtle but consistent, suggesting that more overlap improves crown delineation and hence DBH prediction stability. This also suggests that overlap compensates for lower sensor performance by improving crown delineation.

Understory had minimal impact on DBH estimation. This is demonstrated by prediction accuracy remaining stable across the dashed line (with vs. without understory) in Figure 14. This suggests that crown-based DBH estimation is less sensitive to understory, compared to height or DTM metrics. This is valuable for foresters looking to scale DBH measurement from plot-based to individual tree inventory, as this should remain stable across sites that have different understory conditions.

Lower altitude flights (60 m, grey zones in Figure 14) tended to give better R^2 values than higher altitude (120 m). However, this effect was weaker compared to height or CHM accuracy. This is consistent with DBH depending on lateral crown dimensions rather than vertical precision, which are less sensitive to flight height. The main impact of altitude was seen for DJIL1 at lower overlaps, where the difference was more significant. It is also notable that there was no perceptible influence from flight speed across the flights.

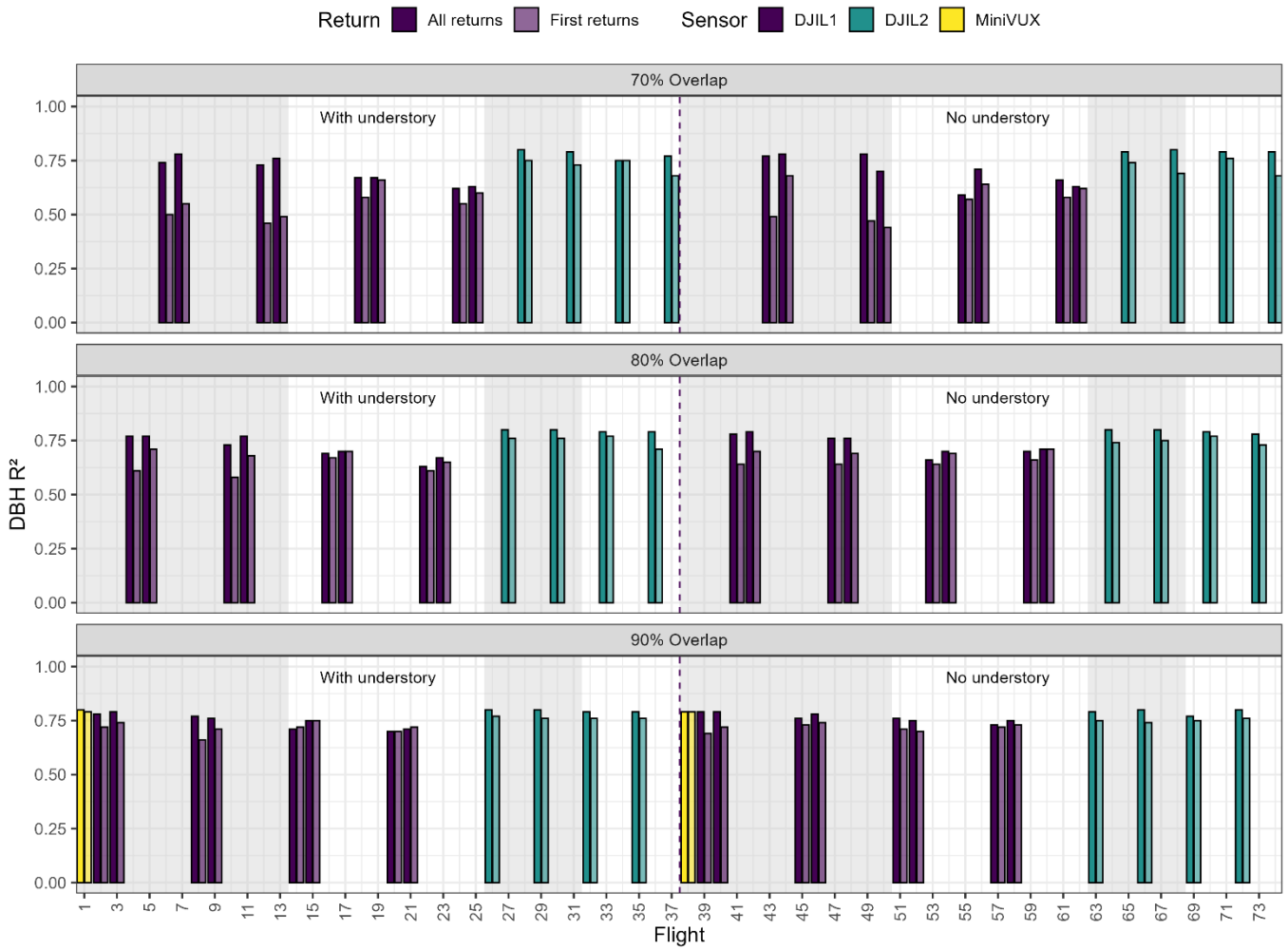

Figure 14. Accuracy of predicting DBH with 3D crown area per flight. The three facets show flights conducted at different overlaps, from top to bottom: 70%, 80%, 90%. Bars show R² of DBH predictions for each flight, coloured by sensor. Darker bars represent analysis of all returns; lighter bars represent first returns only. Grey-shaded panels indicate flights at 60 m AGL; white panels indicate 120 m AGL. Flights to the left of the dashed line were conducted with understory present; flights to the right were conducted with understory removed. Within each altitude-shaded section of the plot, there are two clusters of flights – the first (from left to right) represents flights at 5 m/s, and the second is flights at 10 m/s.

Impact of stocking

Key takeaway: Low stocking improved tree detection accuracy, while high stocking gave the best CHM, DTM, height, and DBH accuracy. The DBH trend at low stocking may reflect crown form changes from late release. Understory had little effect on tree detection/DBH but reduced CHM, DTM, and height accuracy.

When setting up this trial we separated the trees into 4 blocks and thinned the trees within each block to a common industry stocking rate: 833, 1111, and 1667 stems/ha. As 833 had a much lower number of trees, we split this across two stands to maintain more even numbers per treatment. When we analysed the accuracy of metrics across the different stocking rates, some trends emerged:

- **Tree detection accuracy** was most effective on the lowest stocking, declining as stocking increases (Figure 15). This was expected as a lower density stand will have more space between trees, making for a clearer separation of individual tree crowns.
- **CHM and DTM accuracy** were highest for the highest stocked stands (Figure 15). This suggests that denser stands provide more consistent surfaces for canopy and ground modelling.
- **Height accuracy** was also highest for the highest stocking, again suggesting that a fuller canopy is important for accurate height measurements.

Forest Growers Research Ltd, PO Box 1127, Rotorua. Ph: 07 921 1883 Email: forestgrowersresearch@fgr.nz Web: www.fgr.nz

- **DBH accuracy** showed a clear trend with stocking, where the best results were achieved in the highest stocking, and the worst results were from the lowest stocking (Figure 15). This result was unexpected as better separation of tree crowns should improve crown delineation, which should demonstrate a stronger allometric relationship between crown size and DBH. We hypothesise that this is due to the late release of these trees had allowed inter-tree competition to increase the height of the green crown through associated die-off of lower branches, altering the crown form. Further research is needed to test this theory.
- **Presence of understory** showed minimal impact on DBH and ITD accuracy, which was expected as these metrics are more reliant on the upper crown. There was a notable impact on DTM, CHM and height accuracy, however, this was not unexpected, as we have demonstrated that the presence of understory decreases accuracy. Overall, the key takeaway for understory is that it doesn't change the trends observed that are related to stocking.

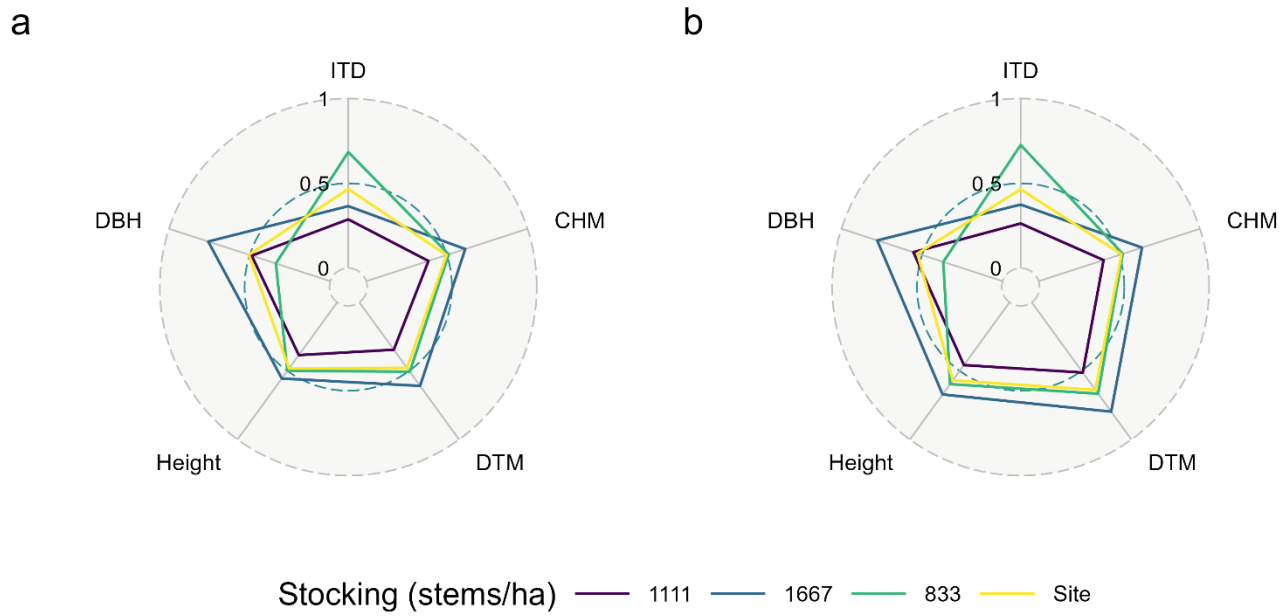

Figure 15. Radar plots demonstrating the impact of stocking on the mean results for accuracy of key metrics: ITD accuracy, CHM and DTM accuracy, height accuracy, and DBH prediction accuracy. Lines radiating from the plot centre represent a normalised scale where 0 is poor and 1 is excellent accuracy. Coloured lines represent the different block stocking rates, and the yellow line shows the combined performance across all blocks. The shape created by each line shows the strengths or weaknesses of these different stocking rates spatially. Panels show relative accuracy of metrics at different stockings for (a) the site with understory, and (b) without understory.

Experiment with non-repetitive scan mode

When choosing the parameters for this optimisation study, adding an additional variable doubled or tripled the volume of datasets to capture and analyse. It was therefore important, given the constraints of the project, to ensure that key variables were selected. "Scan mode" was one of the variables that was identified as an option that was not crucial to data capture, based on advice from other experts in the field, DJI product guidelines, and our own experience. Though it was beyond the scope of this project, we conducted a small trial on a subset of the flight plans with the DJIL2. The results indicated that, when operated in non-repetitive scan mode, DJIL2 performed strongly for DTM and CHM accuracy, showing minimal difference between first and all returns, and minimal impact from speed or altitude. This was not a conclusive test of this parameter, and therefore, further research is needed to test this setting with more confidence. Future research is encouraged to look more closely at this sensor parameter.

Conclusion

In this study, we systematically evaluated flight and sensor parameters, together with key site variables, in a controlled study to assess their impact on key performance metrics and provide guidance for the operational use of industrial-grade ULS in forestry. We found that **altitude was the most influential driver of accuracy**, with lower altitude consistently yielding better results. The **number of returns** had a strong effect on terrain and tree height accuracy, while **overlap** provided consistent benefits, especially for CHM and DBH accuracy. **Flight speed** had a

Forest Growers Research Ltd, PO Box 1127, Rotorua. Ph: 07 921 1883 Email: forestgrowersresearch@fgr.nz Web: www.fgr.nz

smaller effect, though slower flights slightly improved canopy-based metrics. The most decisive factor was **sensor choice**, with DJIL2 outperforming DJIL1 and often performing comparably to the survey-grade MiniVUX sensor.

Our results showed that there was some impact from stocking rate, though further research is required to confirm these trends. Understory had a marked impact on DTM, tree height and CHM accuracy, but minimal impact on tree detection and DBH prediction. Operationally, flight times were mainly driven by overlap, while point density increased with lower altitude, slower speed, higher overlap, and higher scan rate.

Overall, the findings demonstrate that DJIL2 offers a robust, cost-effective solution for forest measurement, though with careful parameter tuning, DJIL1 can still perform competitively. Importantly, this report demonstrates that lidar metrics are not only impacted by flight design, but also by stand structure. As industry increasingly adopts ULS for measuring their forests, it is hoped that this report will guide users to make informed decisions on flight parameters for their specific forest conditions.

Acknowledgements

We would like to thank Jesse Coleman and Jacob Fielding from Kōwhai Aero Ltd for their assistance in capturing data for this project with their DJIL2 sensor. We also thank Richard Vili and Kane Fleet from Scion's Tree Biometrics Field Team, and arborists Andy Neverman, Jesse Coleman and Tom Fowler for thinning the trial for us. We thank Warren Yorston of Scion for surveying the GCPs on the trial site. We are also grateful to Andy Hoult from City Wide Trees for clearing the "understory" trees from the trial site. We would also like to thank Alison Slade and Forest Growers Research for supporting and funding this research, and Michael Watt and Scion Group, Biological Science Institute, for co-funding this research with funds from the Ministry of Business, Innovation and Employment's Strategic Science Investment Fund. We also thank Russell Main, Nicolò Camarretta and Michael Watt of Scion for reviewing this report and providing some useful suggestions for improvement.

References

Apostol, B., Chivulescu, S., Ciceu, A., Petrila, M., Pascu, I.-S., Apostol, E. N., Leca, S., Lorent, A., Tanase, M., & Badea, O. (2007). Data collection methods for forest inventory: a comparison between an integrated conventional equipment and terrestrial laser scanning. *Annals of Forest Research, 50*, 189-202.

CNI Regional YTGEN User Group, N. (2007). PlotSafe: Overlapping feature cruising. Forest inventory procedures.

Dhruva, A., Hartley, R. J., Redpath, T. A., Estarija, H. J. C., Cajes, D., & Massam, P. D. (2024). Effective UAV Photogrammetry for Forest Management: New Insights on Side Overlap and Flight Parameters. *Forests, 15*(12), 2135.

Hartley, R. J. L., Jayathunga, S., Elleouet, J. S., Steer, B. S. C., & Watt, M. S. (2025). UAV-enabled evaluation of forestry plantations: A comprehensive assessment of laser scanning and photogrammetric approaches. *Science of Remote Sensing*, 100245. doi:https://doi.org/10.1016/j.srs.2025.100245

Hu, T., Sun, X., Su, Y., Guan, H., Sun, Q., Kelly, M., & Guo, Q. (2020). Development and performance evaluation of a very low-cost UAV-LiDAR system for forestry applications. *Remote Sensing, 13*(1), 77.

Irwin, L. A., Coops, N. C., Riofrío, J., Grubinger, S. G., Barbeito, I., Achim, A., & Roeser, D. (2025). Prioritizing commercial thinning: quantification of growth and competition with high-density drone laser scanning. *Forestry: An International Journal of Forest Research, 98*(2), 293-307.

Isenburg, M. (2019). LAStools - Efficient LiDAR Processing Software (Version 190404).

Jaakkola, A., Hyyppä, J., Kukko, A., Yu, X., Kaartinen, H., Lehtomäki, M., & Lin, Y. (2010). A low-cost multi-sensoral mobile mapping system and its feasibility for tree measurements. *ISPRS Journal of Photogrammetry and Remote Sensing, 65*(6), 514-522. doi:https://doi.org/10.1016/j.isprsjprs.2010.08.002

Kellner, J. R., Armston, J., Birrer, M., Cushman, K., Duncanson, L., Eck, C., Falleger, C., Imbach, B., Král, K., & Krůček, M. (2019). New opportunities for forest remote sensing through ultra-high-density drone lidar. *Surveys in Geophysics, 40*(4), 959-977.

Koch, B. (2016). Remote sensing supporting national forest assessments. *Knowledge reference for national forest assessments*, 77.

Larjavaara, M., & Muller-Landau, H. C. (2013). Measuring tree height: a quantitative comparison of two common field methods in a moist tropical forest. *Methods in Ecology and Evolution, 4*(9), 793-801. doi:10.1111/2041-210x.12071

Plowright, A., & Roussel, J. (2021). Tools for analyzing remote sensing forest data. doi: https://cran.r-project.org/package=ForestTools.

R Core Team. (2022). R: A language and environment for statistical computing. (Version 4.2.1): R Foundation for Statistical Computing, Vienna, Austria.

Roussel, J.-R., Auty, D., Coops, N. C., Tompalski, P., Goodbody, T. R., Meador, A. S., Bourdon, J.-F., De

Boissieu, F., & Achim, A. (2020). lidR: An R package for analysis of Airborne Laser Scanning (ALS) data. *Remote Sensing of Environment, 251*, 112061. doi:https://doi.org/10.1016/j.rse.2020.112061

Štroner, M., Urban, R., & Línková, L. (2021). A new method for UAV lidar precision testing used for the evaluation of an affordable DJI ZENMUSE L1 scanner. *Remote Sensing, 13*(23), 4811.

Vastaranta, M., Holopainen, M., Haapanen, R., Yu, X., Melkas, T., Hyyppä, J., & Hyyppä, H. (2009). Comparison between an area-based and individual tree detection method for low-pulse density ALS-based forest inventory. *Proceedings of Laser Scanning, Paris, France*, 1-2.

Wallace, L., Lucieer, A., Watson, C., & Turner, D. (2012). Development of a UAV-LiDAR system with application to forest inventory. *Remote Sensing, 4*(6), 1519-1543. doi:10.3390/rs4061519

Wang, Y., Lehtomäki, M., Liang, X., Pyörälä, J., Kukko, A., Jaakkola, A., Liu, J., Feng, Z., Chen, R., & Hyyppä, J. (2019). Is field-measured tree height as reliable as believed – A comparison study of tree height estimates from field measurement, airborne laser scanning and terrestrial laser scanning in a boreal forest. *ISPRS Journal of Photogrammetry and Remote Sensing, 147*, 132-145. doi:10.1016/j.isprsjprs.2018.11.008

Watt, M. S., Jayathunga, S., Hartley, R. J., Pearse, G. D., Massam, P. D., Cajes, D., Steer, B. S., & Estarija, H. J. C. (2024). Use of a Consumer-Grade UAV Laser Scanner to Identify Trees and Estimate Key Tree Attributes across a Point Density Range. *Forests, 15*(6), 899.

Watt, M. S., Jayathunga, S., Mohan, M., Hartley, R. J., Camarretta, N., Steer, B. S., Zhang, W., & Bryson, M. (2025). Predicting Tree-Level Diameter and Volume for Radiata Pine Using UAV LiDAR-Derived Metrics Across a National Trial Series in New Zealand. *Remote Sensing, 17*(8), 1456.

White, J. C., Coops, N. C., Wulder, M. A., Vastaranta, M., Hilker, T., & Tompalski, P. (2016). Remote sensing technologies for enhancing forest inventories: A review. *Canadian Journal of Remote Sensing, 42*(5), 619-641.